JPET # 2016/235069

Title Page

Empagliflozin protects against diet-induced NLRP-3 inflammasome activation and lipid accumulation*

Elisa Benetti, Raffaella Mastrocola, Giovanna Vitarelli, Juan Carlos Cutrin, Debora Nigro, Fausto Chiazza, Eric Mayoux, Massimo Collino, Roberto Fantozzi

Department of Drug Science and Technology (E.B., G.V., F.C., M.C., R.F.), Department of Clinical and Biological Sciences (R.M., D.N.), Department of Biotechnology and Sciences for the Health (J.C.C.), University of Turin, Turin, Italy; Boehringer Ingelheim Pharma, Biberach an der Riss, Germany (E.M.)

Primary laboratory of origin: Department of Drug Science and Technology, University of Turin, Turin, Italy

JPET # 2016/235069

Running Title Page

Running title:

Empagliflozin prevents NLRP-3 inflammasome activation

Corresponding author:

Elisa Benetti, PhD

Dipartimento di Scienza e Tecnologia del Farmaco, University of Turin,

Via Giuria 9, 10125 Turin, Italy

Phone: +39 011 6707689

E-mail address: elisa.benetti@unito.it

- ✓ Number of text pages: 31
- ✓ Number of tables: 1
- ✓ Number of figures: 7
- ✓ Number of references: 44
- ✓ Number of words in the
    - Abstract: 191
    - Introduction: 429
    - Discussion: 1193

Abbreviations

ELISA, enzyme-linked immunosorbent assay; HFHS, high fat high sugar; IL, interleukin; NLRP-3, nucleotide-binding domain, leucine-rich repeat containing protein; OGTT, oral glucose tolerance test; SGLT-2, sodium glucose cotransporter-2; T2DM, type 2 diabetes mellitus.

Abstract

Aim of this study was to evaluate the effects of chronic treatment with empagliflozin, a potent and selective SGLT-2 inhibitor, in a murine model of diet-induced obesity and insulin resistance, focusing on drug effects on body weight reduction and NLRP-3 inflammasome activation, which has never been investigated so far. Male C57BL/6 mice were fed control or a High Fat High Sugar (HFHS) diet for 4 months. Over the last 2 months, subsets of animals were treated with empagliflozin (1-10 mg/kg) added to the diet. Empagliflozin evoked body weight reduction ($p<0.001$ for the highest dose) and positive effects on fasting glycaemia and HOMA IR index. In addition, the drug was able to reduce renal tubular damage and liver triglycerides level in a dose-dependent manner. Interestingly, empagliflozin also decreased cardiac lipid accumulation. Moreover, diet-induced activation of NLRP-3 in kidney and liver (not observed in the heart) was dose-dependently attenuated by empagliflozin. Our results clearly demonstrate the ability of empagliflozin to counteract the deleterious effects evoked by chronic exposure to HFHS diet. Most notably, empagliflozin treatment was associated with NLRP-3 inflammasome signaling modulation, suggesting that this inhibition may contribute to the drug therapeutic effects.

Introduction

In the past decade, compelling data have highlighted the association between metabolic disorders and inflammation (Hotamisligil, 2006; Shoelson et al., 2006). In particular, it has been demonstrated that abdominal obesity is associated with low grade inflammation that leads to insulin resistance and metabolic disorders, thus supporting the recently emerged concept of Type 2 diabetes mellitus (T2DM) as an inflammatory disease (Donath and Shoelson, 2011). One of the most accredited signaling pathways involved in the pathogenesis of obesity-induced insulin resistance is the nucleotide-binding domain, leucine-rich repeat containing protein (NLRP)-3 inflammasome (Davis et al., 2011; Vandanmagsar et al., 2011).

The NLRP-3 inflammasome is a large intracellular multimeric protein danger-sensing platform that promotes the autocatalytic activation of the cysteine protease caspase-1, and mediates the proteolytic activation of pro-inflammatory cytokines, including pro-interleukin (IL)-1β (Lamkanfi, 2011).

We and others have previously demonstrated that the NLRP-3 inflammasome contributes to the metabolic abnormalities described in the pathogenesis of obesity-induced insulin resistance and its pharmacological or genetic modulation exerts protective effects against adiposity increase and insulin resistance (Stienstra et al., 2011; Chiazza et al., 2015). In particular, a causal role for IL-1β in this scenario has been recognized and its contribution to the impairment of insulin signaling and to the onset and/or maintenance of insulin resistance is well known (Larsen et al., 2007; Dinarello, 2009). Interestingly, the activation of NLRP-3 in T2DM pathogenesis is further supported by recent evidence that treatment with metformin, the most widely prescribed oral antihyperglycemic agent, triggers inhibition of caspase-1 cleavage and IL-1β maturation in monocyte-derived macrophages from diabetic patients (Lee et al., 2013).

Inhibitors of the sodium glucose cotransporter (SGLT)-2 are a novel class of antidiabetic drugs (Idris and Donnelly, 2009). SGLT-2 is located on the apical side of the proximal tubular cells and accounts for the majority (about 90%) of glucose reabsorption in the kidney (Wright, 2001). Inhibition of SGLT-2 activity increases glucose excretion, thus lowering blood glucose level (Bakris et al., 2009). Due to their insulin-independent mode of action, SGLT-2 inhibitors are an attractive pharmacological strategy, distinct from traditional oral anti-diabetic therapies. Moreover, administration of these drugs is associated with additional beneficial effects including body weight loss (Kurosaki and Ogasawara, 2013; Monami et al., 2014).

Some studies have demonstrated that SGLT-2 inhibitors could counteract inflammation associated with diabetic conditions in kidney (Gembardt et al., 2014; Vallon et al., 2014) and liver organs (Tahara et al., 2013) of Akita or type 2 diabetic mice. However, to date, the effects of SGLT-2 inhibitors on NLRP-3 inflammasome activation have not been described.

The aim of this study was to evaluate the effects of empagliflozin, a potent and selective SGLT-2 inhibitor (Grempler et al., 2012), in a murine model of obesity and insulin resistance induced by a diet.

The research was focused on drug effects against body weight increase, and on the potential drug ability to affect NLRP-3 inflammasome-activation in the target organs of obesity/diabetic diseases.

Material and Methods

Animals and experimental procedures

Four-week-old male C57Bl6/J mice (n=120, provided by Charles River, Lecco, Italy) were housed in a controlled environment at 25±2°C with alternating 12-h light and dark cycles and fed normal diet during a 1 week adaptation period. The animals were then randomly (1:2) allocated in two experimental groups: mice fed a control diet or a High Fat-High Sugar (HFHS) diet for 8 weeks. The HFHS diet (D12451) contained 45% kcal fat (lard and soybean oil), 20% protein (casein), 35% carbohydrate (fructose 55% and glucose 45%) (D12451, ssniff Spezialdiäten GmbH, Ferdinand-Gabriel-Weg, Germany). Animals were then randomly allocated in six groups (n= 20): Control group (Control), Control group+empagliflozin 10 mg/kg (C+E10), HFHS group (HFHS), HFHS+empagliflozin 1 mg/kg (HFHS+E1), HFHS+empagliflozin 3 mg/kg (HFHS+E3), HFHS+empagliflozin 10 mg/kg (HFHS+E10). Empaglifozin mixed in diet at different titrations was chosen to deliver a daily dosage of approximately 1, 3 and 10 mg/kg in regard to proven improvement of glycaemia and feature of metabolic syndrome in diabetic rats (Thomas et al., 2012).

The animal protocol has been carried out in accordance with the European Directive 2010/63/EU as well as the Guide for the Care and Use of Laboratory Animals as adopted and promulgated by the U.S. National Institutes of Health, and was approved by the local ethical committee.

Food intake determination

Every week 200/250 grams of foods were placed in every cage. Food intake was measured by dividing the food consumption for the number of animals present in the cage.

Oral glucose tolerance test (OGTT)

The day before sacrifice, after a fasting period of 16 hours, OGTT was performed. Once before glucose administration (2 g/kg by oral gavage), and 15, 30, 60, 120 and 180 min afterwards, blood samples were obtained from the saphenous vein puncture, and glucose concentration was determined with a conventional Glucometer (Glucomen LX Plus, A. Menarini Diagnostics, Florence, Italy).

Biochemical analysis

At the end of the study (week 16), after 16h fasting period, the mice were anesthetized using isoflurane via an anesthesia machine (IsoFlo, Abbott Laboratories, Chicago, IL, USA) and sacrificed by cardiac puncture/exsanguination. Glycemia was measured using the GlucoMen LX kit. Plasma lipid profiles were determined by measuring the content of triglycerides (TGs), total cholesterol, high-density-lipoprotein (HDL) by using commercial reagent kits (Hospitex diagnostics, Florence, Italy). LDL was determined by calculation [LDL = total cholesterol – (HDL + TG/5)]. Plasma insulin and tissue IL-1β levels were measured using enzyme-linked immunosorbent assay (ELISA) kits (Quantikine ELISA Kit, R&D Systems, Minneapolis, MN, USA). Urinary albumin excretion was evaluated and expressed as albumin-to-creatinine ratio (ACR) in 18 hours urine collection (Mouse Albumin ELISA Quantitation Set, Bethyl Laboratories, Montgomery, TX, USA; Creatinine Colorimetric Assay Kit, Cayman Chemical, Ann Arbor, MI, USA).

Tissue extracts

Kidney, liver and cardiac apex extracts were prepared as previously described (Benetti et al., 2013). Briefly, tissues were homogenized and centrifuged. Supernatants were removed and the protein content was determined using a BCA protein assay following the manufacturer's instructions (Pierce Biotechnology Inc. Rockford, IL, USA).

Western blot analysis

About 60 µg total proteins were loaded for Western blot experiments as previously described (Collino et al., 2013). The membranes were stripped and incubated with β-actin/tubulin monoclonal antibody to assess gel-loading homogeneity.

Histopathological examination

Sagittal sections of both kidneys and fragments from the left lateral and medial lobes of livers were fixed in 4% buffered formaldehyde solution overnight at 4° C. Dewaxed 5 µm sections were stained with hematoxylin-eosin and examined under an Olympus Bx4I microscope (40x magnification) with an AxioCamMR5 photographic attachment. Vacuolar degeneration of renal contort proximal tubules was classified as light (<10% of tubules with vacuolar degeneration), moderate (10-20%) and severe (>20%). The level of macrovesicular/microvesicular hepatic steatosis was evaluated according to the following grading: light (<30% hepatocytes with macrovesicles/microvesicles), moderate (31-60%) and severe (>60%).

Heart Oil Red staining

Neutral lipids were assessed on frozen sections of cardiac apex (10 µm in thickness) by Oil Red O staining using an Olympus Bx4I microscope (40x magnification) with an AxioCamMR5 photographic attachment (Zeiss, Gottingen, Germany).

TGs level

Hepatic and cardiac TGs were extracted from total tissue homogenates of randomly selected animals and assayed using reagent kits according to the manufacturer's instructions (Triglyceride Quantification Kit, Abnova Corporation, Aachen, Germany).

Materials

Unless otherwise stated, all compounds were purchased from the Sigma-Aldrich Company Ltd. (St. Louis, MO, USA). PVDF was from Millipore Corporation (Bedford, MA, USA). Primary Antibodies were from Epitomics-Abcam Company (Cambridge, UK), Adipogene

(Liestal Switzerland) and Sigma for NLRP-3 (1:5000), caspase 1 p-20 (1µl/ml) and β-actin (1:1000), respectively. Secondary Antibodies were from Cell-Signaling Technology (1:5000, Beverly, MA, USA) and Luminol ECL from PerkinElmer (Waltham, MA, USA).

Statistical analysis

All values in both the text and figures are expressed as mean ± SEM for *n* observations. One-way or Two-way analysis of variance with Bonferroni's post-hoc test (when applicable) was performed using the GraphPad Prism version 5.0 for Windows (GraphPad Software, San Diego, CA, USA) and p values below 0.05 were considered as significant.

Results

Effect of empagliflozin on the diet-induced body weight increase

Average body weight of HFHS mice was higher than that recorded in the control group throughout the experiment ($p<0.001$ vs HFHS, Figure 1A).

At the end of the study (week 16) the body weights were 25.17±0.76 g (ΔBW=+13.54% *vs* week 8), and 34.59±3.03 g (ΔBW+22.58% *vs* week 8) for the control and HFHS groups, respectively.

In comparison to HFHS animals, a lower body weight was recorded in empagliflozin-treated groups: 33.49±3.39g (ΔBW=+17.73% *vs* week 8); 33.92±4.58g (ΔBW=+18.01%) and 31.24±2.46g (ΔBW=+9.97%) for HFHS+E1, HFHS+E3 and HFHS+E10 respectively, albeit only the highest dose evoked statistically significant differences ($p<0.001$ *vs* HFHS group). Notably, the average body weight gain in mice treated with the highest dose of empagliflozin (10 mg/kg) was similar to that recorded in the control group (2.83 *vs* 3.1, weeks 16-8), thus meaning that the highest dose abolished the weight gain effects of the HFHS diet. No effects on BW were observed when the drug was administered to animals on control diet (Figure 1A). Empagliflozin did not affect food intake (Figure 1B).

Interestingly, in animals fed with HFHS diet the efficiency of food intake (defined as the body weight gain divided by the food intake) was decreased by empagliflozin especially at the highest dose ($p<0.001$ Table 1). In HFHS animals, the highest dose of empagliflozin showed a clear reduction in epididymal fat ($p<0.001$ *vs* HFHS group) and liver weight ($p>0.05$ *vs* control group).

Effect of empagliflozin on fasting glycaemia, OGTT test and blood chemistry

At the end of the study (week 16), compared to control, chronic exposure to HFHS diet resulted in significant 45% and 80% increase in fasting serum glucose and insulin levels,

respectively (Table 1). As expected, empagliflozin treatment significantly reduced glycaemia in a dose-dependent manner, whereas the effect on insulin levels was modest and not statistically significant.

HOMA IR index increased three-fold in HFHS animals *vs* Control animals ($p<0.001$), and a significant reduction was evoked by empagliflozin at all the tested doses (Table 1).

Empagliflozin did not affect the diet-induced increase of plasma tot-cholesterol and LDL-cholesterol levels.

The fasting glucose, over time of experimentation, was highlighted in Figure 2A. Chronic exposure to HFHS diet caused an increase in fasting glycaemia since the first month of diet manipulation, reaching the maximum level after two months ($p<0.001$ *vs* Control). Empagliflozin significantly improved glycaemic control at each test dose already after the first month of drug administration (Figure 2A).

In addition, HFHS diet caused a deterioration of glucose tolerance (OGTT, Figure 2B) in comparison to control diet ($AUC_{HFHS} > AUC_{control}$). As shown in Figure 2b-2c, compared to HFHS group, empagliflozin 10 mg/kg exerted a significant improvement of glucose tolerance ($AUC_{0\text{-}180min}$: $p<0.05$ *vs* HFHS, Figure 2C).

Effect of empagliflozin on diet-induced renal damage

As shown in Figure 3A, HFHS diet was associated with a severe vacuolar degeneration of the tubular epithelial cells of the S1-S2 of the contorted proximal tubules. Drug treatment attenuated damage severity in a dose-dependent manner (the effect of the highest dose is displayed in the picture).

Compared to control mice, HFHS animals showed a significant increase in the albumin-to-creatinine ratio (ACR), thus confirming renal dysfunction (D'Amico and Bazzi, 2003). Empagliflozin significantly counteracted this effect at all the tested doses (Figure 3B).

Effect of empagliflozin on renal NLRP-3 inflammasome activation

As shown in Figure 4, kidneys from HFHS mice showed both NLRP-3 over-expression (Figure 4A) and caspase-1 activation as indicated by the appearance of the p20 subunit of caspase-1 (Figure 4B). The end-product of NLRP-3 inflammasome activation, the mature cytokine IL-1β, was significantly increased in the kidneys of HFHS mice, in comparison with control animals (Figure 4C). Both, caspase 1 activation and IL-1β production were decreased in kidneys from HFHS mice treated with empagliflozin. In particular, the effect was statistically significant for empagliflozin at doses of 3 mg/kg and 10 mg/kg.

Effect of empagliflozin on diet-induced liver damage

HFHS feeding produced a severe mixed fatty change in terms of hepatocytes with micro and macrovacuoles. They were detected predominantly in the periportal zones of the acini. When mice were treated with empagliflozin, the degree of steatosis was attenuated and the number of hepatocytes with lipid droplets was markedly reduced (higher dose effect represented in Figure 5A). HFHS animals displayed a four-fold increase in hepatic triglycerides measured in liver homogenates and this value was dose-dependently decreased by the drug (Figure 5B).

Effect of empagliflozin on hepatic diet-induced NLRP-3 inflammasome activation

To further investigate the empagliflozin effect on liver, we evaluated whether hepatic steatosis was correlated with diet-induced NLRP-3 inflammasome activation and the ability of the drug to modulate this signaling pathway.

In comparison to HFHS animals, drug treatment was dose-dependently associated to a decrease of NLRP-3 expression (Figure 6A), with a significant effect also to caspase-1 activation by the highest dose (Figure 6B). The effect on inflammasome pathway resulted in a consequent dese-dependent reduction in IL-1β production (Figure 6C). The effect was statistically significant at 10 mg/kg ($p<0.05$ *vs* HFHS).

Effect of empagliflozin on cardiac lipid accumulation and NLRP-3 inflammasome

Concurrent with the development of hepatic steatosis, HFHS animals displayed evident lipid deposition in the heart (Figure 7A). As shown by Oil Red O staining (Figure 7A), cytoplasmic micro- or macrovacuolar lipid droplets were detected in animal fed the HFHS diet. Empagliflozin administration attenuated fat accumulation and this effect was confirmed by a significant diminution of TG content (Figure 7B), already evident at 1 mg/kg.

In contrast to the effects of HFHS diet in kidney and liver, we did not detect NLRP-3 overexpression and caspase-1 activation in the heart (data not shown), as well as an increase of cardiac IL-1β production (Figure 7C). In this condition treatment with empagliflozin did not affect the cardiac NLRP-3 signaling pathway.

Discussion

This study investigates, for the first time, the effects of the SGLT-2-selective inhibitor empagliflozin on the activation of NLRP-3 inflammasome pathway in a murine model of diet-induced obesity and insulin resistance. So far, the effect of empagliflozin has been tested in diabetic models that exhibit obvious hyperglycemia and insulin resistance for genetic manipulation [Akyta mice (Vallon et al., 2014), ob/ob (Gembardt F et al., 2014), Zucker rat (Thomas et al., 2012)] and no studies have been performed in models where the pathological features (hyperglycemia, insulin resistance and oversize) are due to an unhealthy life style (i.e. hypercaloric diet and sedentary life), closely resembling changes observed in human with type 2 diabetes (Panchal et al., 2011).

Drug administration started after two months of diet manipulation, when the detrimental effects of HFHS diet on metabolic parameters (e.g. body weight, blood glucose level) were established. This “therapeutic” design was chosen to enhance validity and fidelity of our model, thus allowing a superior translatability.

According to literature (Liakos et al., 2014), empagliflozin treatment was associated with weight loss especially at the dose of 10mg/kg. A that dose the body weight gain of animals under HFHF diet was comparable to animals with chow diet.

In our study, no compensatory increase in food intake was observed in animals treated with empagliflozin, in contrast to results obtained in diet-induced obese rats treated with dapagliflozin (Devenny et al., 2012).

Empagliflozin showed a marked ability to decrease fasting glycaemia and a modest, but still significant, effect on OGTT performed in fasted animals. In addition, empagliflozin significantly prevented diet-induced increase of HOMA-IR index, a well recognized marker

of insulin resistance, thus supporting data indicating that SGLT-2 inhibition attenuates the hyperglicemia-induced decline in insulin sensitivity (Rossetti et al., 1987; Musso et al., 2012).

Drug treatment was also associated with a reduction of triglycerides accumulation in liver and heart. Microscopic observations confirm that empagliflozin decreased morphological alterations associated with steatotis in these two tissues. Such effect on liver triglycerides was previously reported with another SGLT-2 inhibitor, ipragliflozin, in a similar experimental model, thus suggesting that SGLT-2 inhibition could be useful to prevent the establishment of nonalcoholic fatty liver disease (NAFLD) in type 2 diabetes (Tahara et al., 2013).

Interestingly, our study is the first one demonstrating that a SGLT-2 inhibitor counteracts the diet-induced cardiac fat accumulation. This observation could help to explain the improvement in cardiovascular injury and remodeling induced by the drug in ob/ob mice (Lin et al., 2014). Levelt et al., demonstrated that myocardial steatosis is a predictor of concentric LV (left ventricle) remodeling and a prominent and early feature of diabetic cardiomyopathy (Levelt et al., 2016). Therefore, strategies aimed at reversing myocardial steatosis may potentially improve prognosis in patients with diabetes.
On this basis, empagliflozin ability to counteract cardiac fatty acid accumulation may contribute, at least in part, to prevent cardiovascular event in type 2 diabetic patients, as recently reported in the Empa-Reg Outcome study (Zinman et al., 2015).

Empagliflozin treatment caused a decrease in pathological cell alterations in the kidneys of mice fed the HFHS diet. In accordance with previous papers (Janigan and Santamaria, 1961; Trump and Janigan, 1962), we observed that a chronic exposure to a diet enriched in sugars caused swelling and vacuolization of the proximal tubular cells, thus producing a

morphological pattern known as “osmotic nephrosis”. Empagliflozin dose-dependently decreased the tubular damage, specifically the diet-induced tubular vacuolation, an early manifestation of tubular degeneration (Frazier et al., 2012). Morphological improvement was associated with the beneficial effects on renal function, as showed by ability of the drug to prevent diet-induced ACR increase. The effects on tubular damage and ACR are likely secondary to glycaemic control (Vallon et al., 2014).

To better elucidate the molecular mechanism(s) underlying the beneficial effects associated with empagliflozin treatment, we focused our investigation on the NLRP-3 inflammasome, a protein complex involved in the development of obesity-induced insulin resistance. In keeping with our previous studies (Collino et al., 2013) (Chiazza et al., 2015), here we confirm that hypercaloric diets induce NLRP-3 inflammasome activation in several organs, including liver and kidney. Interestingly, for the first time, this study demonstrates that animals treated with empagliflozin showed a decrease of NLRP-3 activation. The final point of this effect, namely the IL-1β production, was dose-dependently reduced in both kidney and liver, thus suggesting that drug beneficial effects are not limited to its target organ.

Renal NLRP-3 inflammasome inhibition has been suggested to counteract development of diabetic nephropathy and chronic kidney disease (Anders and Muruve, 2011; Chen et al., 2013; Wada and Makino, 2016), and its inhibition in the liver may exert further beneficial effects, such as reducing the progression of hepatic steatosis to more severe forms, including steatohepatitis (Wree et al., 2014). In the liver, we found an interesting correlation between the dose-dependent decrease of TGs and IL-1β induced by the drug. These effects could be related to the ability of IL-1β to induce hepatic TG accumulation. In keeping with this hypothesis Negrin et al., (Negrin et al., 2014) shown that IL-1β treatment increases hepatic fat

accumulation in primary mouse hepatocytes and that pharmacological inhibition of IL-1 signaling attenuated obesity-induced hepatic steatosis. These data suggest a crucial role of NLRP-3 activation in the pathogenesis of liver steatosis. Taken together, these findings indicate that empagliflozin treatment may exerts indirect effects related to NLRP-3 inflammasome activation, beyond the improvement of glycemic control, glucose tolerance and insulin resistance.

As also metformin has been previously shown to attenuate inflammasome–mediated caspase-1 activation (Lee et al., 2013), we may speculate that the modulation of the NLRP-3/IL-1β pathway associated with glucose lowering effect can significantly contribute to the beneficial therapeutic effects of antidiabetic drugs.

Although the NLRP-3 inflammasome is known to affect metabolic derangements in insulin-sensitive tissues, its role in the heart suffering diet-induced pathogenic alterations has not been previously investigated. Our data show that myocardial steatosis observed in HFHS animals is not associated with local NLRP-3-induced IL-1β production. In contrast to other conditions, i.e ischemia/reperfusion injury (Mastrocola et al., 2016), infections (Wang et al., 2014) or diabetic cardiomyopathy (Luo et al., 2014), our study shows, for the first time, that this pathway is not activated in the cardiac tissue of animal fed HFHS diet.

In addition, in patients with metabolic syndrome Muniyappa et al. (Muniyappa et al., 2015), demonstrated that hepatic and peripheral index of insulin sensitivity were negative related to hepatic fat content, but unrelated to myocardial fat accumulation, thus suggesting that the correlation between fat accumulation and insulin resistance is very strong in some tissues, such as liver, but not in the heart. This finding is consistent with the different response in NLRP-3 activation that we found between liver and heart.

Finally, we found that treatment with empagliflozin had not any effects on NLRP-3 signaling pathway in control animals. Despite we do not know if it is possible to decrease the activity of NLRP-3 under basal conditions, this lack of effect could suggest that this drug not exerts a direct inhibition on NLRP-3 inflammasome.

In summary, empagliflozin attenuated in a dose-dependent manner the metabolic abnormalities induced by chronic exposure to an hypercaloric diet by abolishing the diet-induced body weight increase, improving hyperglycemia, diminishing liver and cardiac steatosis, and decreasing the tissue injury associated with obesity and insulin resistance.

Interestingly, empagliflozin reduced in a dose-dependent manner the diet-induced activation of NLRP-3 inflammasome pathway in kidney and liver. Neither the diet manipulation nor the drug treatment affected myocardial NLRP-3 inflammasome pathway.

To our knowledge, this is the first paper that investigated the effect of a SGLT-2 inhibitor on diet-induced NLRP-3 inflammasome activation and myocardial fat accumulation, thus adding an original piece of evidence to the effects correlated with this new class of drugs.

Acknowledgments

We thanks Dr. Arianna Carolina Rosa and Dr. Gianluca Miglio for their support.

Authorship Contributions

Participated in research design: Benetti

Conducted experiments: Benetti, Mastrocola, Vitarelli, Cutrin, Nigro, Chiazza, Collino

Performed data analysis: Benetti, Mastrocola, Cutrin

Wrote or contributed to the writing of the manuscript: Benetti, Collino, Mayoux, Fantozzi

All authors have approved the final version of the manuscript.

Conflict of interest

Eric Mayoux is the employee of Boehringer Ingelheim Pharma GmbH & Co. KG.

References

Anders HJ and Muruve DA (2011) The inflammasomes in kidney disease. *Journal of the American Society of Nephrology : JASN* **22**:1007-1018.

Bakris GL, Fonseca VA, Sharma K and Wright EM (2009) Renal sodium-glucose transport: role in diabetes mellitus and potential clinical implications. *Kidney international* **75**:1272-1277.

Benetti E, Mastrocola R, Rogazzo M, Chiazza F, Aragno M, Fantozzi R, Collino M and Minetto MA (2013) High sugar intake and development of skeletal muscle insulin resistance and inflammation in mice: a protective role for PPAR- delta agonism. *Mediators of inflammation* **2013**:509502.

Chen K, Zhang J, Zhang W, Zhang J, Yang J, Li K and He Y (2013) ATP-P2X4 signaling mediates NLRP3 inflammasome activation: a novel pathway of diabetic nephropathy. *The international journal of biochemistry & cell biology* **45**:932-943.

Chiazza F, Couturier-Maillard A, Benetti E, Mastrocola R, Nigro D, Cutrin JC, Serpe L, Aragno M, Fantozzi R, Ryffel B, Thiemermann C and Collino M (2015) Targeting the NLRP3 inflammasome to reduce diet-induced metabolic abnormalities in mice. *Molecular medicine*.

Collino M, Benetti E, Rogazzo M, Mastrocola R, Yaqoob MM, Aragno M, Thiemermann C and Fantozzi R (2013) Reversal of the deleterious effects of chronic dietary HFCS-55 intake by PPAR-delta agonism correlates with impaired NLRP3 inflammasome activation. *Biochemical pharmacology* **85**:257-264.

D'Amico G and Bazzi C (2003) Pathophysiology of proteinuria. *Kidney international* **63**:809-825.

Davis BK, Wen H and Ting JP (2011) The inflammasome NLRs in immunity, inflammation, and associated diseases. *Annual review of immunology* **29**:707-735.

Devenny JJ, Godonis HE, Harvey SJ, Rooney S, Cullen MJ and Pelleymounter MA (2012) Weight loss induced by chronic dapagliflozin treatment is attenuated by compensatory hyperphagia in diet-induced obese (DIO) rats. *Obesity* **20**:1645-1652.

Dinarello CA (2009) Immunological and inflammatory functions of the interleukin-1 family. *Annual review of immunology* **27**:519-550.

Donath MY and Shoelson SE (2011) Type 2 diabetes as an inflammatory disease. *Nature reviews Immunology* **11**:98-107.

Frazier KS, Seely JC, Hard GC, Betton G, Burnett R, Nakatsuji S, Nishikawa A, Durchfeld-Meyer B and Bube A (2012) Proliferative and nonproliferative lesions of the rat and mouse urinary system. *Toxicologic pathology* **40**:14S-86S.

Gembardt F, Bartaun C, Jarzebska N, Mayoux E, Todorov VT, Hohenstein B and Hugo C (2014) The SGLT2 inhibitor empagliflozin ameliorates early features of diabetic nephropathy in BTBR ob/ob type 2 diabetic mice with and without hypertension. *American journal of physiology Renal physiology* **307**:F317-325.

Grempler R, Thomas L, Eckhardt M, Himmelsbach F, Sauer A, Sharp DE, Bakker RA, Mark M, Klein T and Eickelmann P (2012) Empagliflozin, a novel selective sodium glucose cotransporter-2 (SGLT-2) inhibitor: characterisation and comparison with other SGLT-2 inhibitors. *Diabetes, obesity & metabolism* **14**:83-90.

Hotamisligil GS (2006) Inflammation and metabolic disorders. *Nature* **444**:860-867.

Idris I and Donnelly R (2009) Sodium-glucose co-transporter-2 inhibitors: an emerging new class of oral antidiabetic drug. *Diabetes, obesity & metabolism* **11**:79-88.

Janigan DT and Santamaria A (1961) A histochemical study of swelling and vacuolation of proximal tubular cells in sucrose nephrosis in the rat. *The American journal of pathology* **39**:175-193.

Kurosaki E and Ogasawara H (2013) Ipragliflozin and other sodium-glucose cotransporter-2 (SGLT2) inhibitors in the treatment of type 2 diabetes: preclinical and clinical data. *Pharmacology & therapeutics* **139**:51-59.

Lamkanfi M (2011) Emerging inflammasome effector mechanisms. *Nature reviews Immunology* **11**:213-220.

Larsen CM, Faulenbach M, Vaag A, Volund A, Ehses JA, Seifert B, Mandrup-Poulsen T and Donath MY (2007) Interleukin-1-receptor antagonist in type 2 diabetes mellitus. *The New England journal of medicine* **356**:1517-1526.

Lee HM, Kim JJ, Kim HJ, Shong M, Ku BJ and Jo EK (2013) Upregulated NLRP3 inflammasome activation in patients with type 2 diabetes. *Diabetes* **62**:194-204.

Levelt E, Mahmod M, Piechnik SK, Ariga R, Francis JM, Rodgers CT, Clarke WT, Sabharwal N, Schneider JE, Karamitsos TD, Clarke K, Rider OJ and Neubauer S (2016) Relationship Between Left Ventricular Structural and Metabolic Remodeling in Type 2 Diabetes. *Diabetes* **65**:44-52.

Liakos A, Karagiannis T, Athanasiadou E, Sarigianni M, Mainou M, Papatheodorou K, Bekiari E and Tsapas A (2014) Efficacy and safety of empagliflozin for type 2 diabetes: a systematic review and meta-analysis. *Diabetes, obesity & metabolism* **16**:984-993.

Lin B, Koibuchi N, Hasegawa Y, Sueta D, Toyama K, Uekawa K, Ma M, Nakagawa T, Kusaka H and Kim-Mitsuyama S (2014) Glycemic control with empagliflozin, a novel selective SGLT2 inhibitor, ameliorates cardiovascular injury and cognitive dysfunction in obese and type 2 diabetic mice. *Cardiovascular diabetology* **13**:148.

Luo B, Li B, Wang W, Liu X, Liu X, Xia Y, Zhang C, Zhang Y, Zhang M and An F (2014) Rosuvastatin alleviates diabetic cardiomyopathy by inhibiting NLRP3 inflammasome and MAPK pathways in a type 2 diabetes rat model. *Cardiovascular drugs and therapy / sponsored by the International Society of Cardiovascular Pharmacotherapy* **28**:33-43.

Mastrocola R, Collino M, Penna C, Nigro D, Chiazza F, Fracasso V, Tullio F, Alloatti G, Pagliaro P and Aragno M (2016) Maladaptive Modulations of NLRP3 Inflammasome and Cardioprotective Pathways Are Involved in Diet-Induced Exacerbation of Myocardial Ischemia/Reperfusion Injury in Mice. *Oxidative medicine and cellular longevity* **2016**:3480637.

Monami M, Nardini C and Mannucci E (2014) Efficacy and safety of sodium glucose co-transport-2 inhibitors in type 2 diabetes: a meta-analysis of randomized clinical trials. *Diabetes, obesity & metabolism* **16**:457-466.

Muniyappa R, Noureldin R, Ouwerkerk R, Liu EY, Madan R, Abel BS, Mullins K, Walter MF, Skarulis MC and Gharib AM (2015) Myocardial Fat Accumulation Is Independent of Measures of Insulin Sensitivity. *The Journal of clinical endocrinology and metabolism* **100**:3060-3068.

Musso G, Gambino R, Cassader M and Pagano G (2012) A novel approach to control hyperglycemia in type 2 diabetes: sodium glucose co-transport (SGLT) inhibitors: systematic review and meta-analysis of randomized trials. *Annals of medicine* **44**:375-393.

Negrin KA, Roth Flach RJ, DiStefano MT, Matevossian A, Friedline RH, Jung D, Kim JK and Czech MP (2014) IL-1 signaling in obesity-induced hepatic lipogenesis and steatosis. *PloS one* **9**:e107265.

Panchal SK, Poudyal H, Iyer A, Nazer R, Alam A, Diwan V, Kauter K, Sernia C, Campbell F, Ward L, Gobe G, Fenning A and Brown L (2011) High-carbohydrate high-fat diet-induced metabolic syndrome and cardiovascular remodeling in rats. *Journal of cardiovascular pharmacology* **57**:51-64.

Rossetti L, Smith D, Shulman GI, Papachristou D and DeFronzo RA (1987) Correction of hyperglycemia with phlorizin normalizes tissue sensitivity to insulin in diabetic rats. *The Journal of clinical investigation* **79**:1510-1515.

Shoelson SE, Lee J and Goldfine AB (2006) Inflammation and insulin resistance. *The Journal of clinical investigation* **116**:1793-1801.

Stienstra R, van Diepen JA, Tack CJ, Zaki MH, van de Veerdonk FL, Perera D, Neale GA, Hooiveld GJ, Hijmans A, Vroegrijk I, van den Berg S, Romijn J, Rensen PC, Joosten LA, Netea MG and Kanneganti TD (2011) Inflammasome is a central player in the induction of obesity and insulin resistance. *Proceedings of the National Academy of Sciences of the United States of America* **108**:15324-15329.

Tahara A, Kurosaki E, Yokono M, Yamajuku D, Kihara R, Hayashizaki Y, Takasu T, Imamura M, Li Q, Tomiyama H, Kobayashi Y, Noda A, Sasamata M and Shibasaki M (2013) Effects of SGLT2 selective inhibitor ipragliflozin on hyperglycemia, hyperlipidemia, hepatic steatosis, oxidative stress, inflammation, and obesity in type 2 diabetic mice. *European journal of pharmacology* **715**:246-255.

Thomas L, Grempler R, Eckhardt M, Himmelsbach F, Sauer A, Klein T, Eickelmann P and Mark M (2012) Long-term treatment with empagliflozin, a novel, potent and selective SGLT-2 inhibitor, improves glycaemic control and features of metabolic syndrome in diabetic rats. *Diabetes, obesity & metabolism* **14**:94-96.

Trump BF and Janigan DT (1962) The pathogenesis of cytologic vacuolization in sucrose nephrosis. An electron microscopic and histochemical study. *Laboratory investigation; a journal of technical methods and pathology* **11**:395-411.

Vallon V, Gerasimova M, Rose MA, Masuda T, Satriano J, Mayoux E, Koepsell H, Thomson SC and Rieg T (2014) SGLT2 inhibitor empagliflozin reduces renal growth and albuminuria in proportion to hyperglycemia and prevents glomerular hyperfiltration in diabetic Akita mice. *American journal of physiology Renal physiology* **306**:F194-204.

Vandanmagsar B, Youm YH, Ravussin A, Galgani JE, Stadler K, Mynatt RL, Ravussin E, Stephens JM and Dixit VD (2011) The NLRP3 inflammasome instigates obesity-induced inflammation and insulin resistance. *Nature medicine* **17**:179-188.

Wada J and Makino H (2016) Innate immunity in diabetes and diabetic nephropathy. *Nature reviews Nephrology* **12**:13-26.

Wang Y, Gao B and Xiong S (2014) Involvement of NLRP3 inflammasome in CVB3-induced viral myocarditis. *American journal of physiology Heart and circulatory physiology* **307**:H1438-1447.

Wree A, McGeough MD, Pena CA, Schlattjan M, Li H, Inzaugarat ME, Messer K, Canbay A, Hoffman HM and Feldstein AE (2014) NLRP3 inflammasome activation is required for fibrosis development in NAFLD. *Journal of molecular medicine* **92**:1069-1082.

Wright EM (2001) Renal Na(+)-glucose cotransporters. *American journal of physiology Renal physiology* **280**:F10-18.

Zinman B, Wanner C, Lachin JM, Fitchett D, Bluhmki E, Hantel S, Mattheus M, Devins T, Johansen OE, Woerle HJ, Broedl UC, Inzucchi SE and Investigators E-RO (2015) Empagliflozin, Cardiovascular Outcomes, and Mortality in Type 2 Diabetes. *The New England journal of medicine* **373**:2117-2128.

Footnotes

* Funding

This work was supported by Boehringer Ingelheim International GmbH

Figure Legends

Figure 1 Effects of diet manipulation and empagliflozin treatment on mice body weight.

Body weight (panel A) and food intake (panel B) of mice were measured every week during diet manipulation (1-16 weeks) and drug treatment (9-16 weeks). Values are means ± SEM for n= 20 animals per group. At the end of week 1, weights of all HFHS groups are statistically different from control groups ($p<0.001$). #$p<0.05$ *vs* HFHS; ###$p<0.01$ *vs* HFHS; ***$p<0.001$ *vs* C.

Figure 2 Effects of diet manipulation and empagliflozin treatment on fasting glycemia (panel A), and oral glucose tolerance test (OGTT, panel B and AUC, panel C).

Blood glycemia was measured every month, whereas OGTT test was performed at the end of the experimental protocol (week 16) in fasted animals. Values are means±SEM for n= 15 randomly selected animals per group. *$p<0.05$, **$p<0.01$, ***$p<0.001$ *vs* C; #$p<0.05$; ##$p<0.01$ *vs* HFHS.

Figure 3 Effects of empagliflozin treatment on diet-induced kidney injury.

Representative microphotographs (×200 magnification) of hematoxylin-eosin stained kidney sections from control and HFHS animals untreated or treated with empagliflozin 10 mg/kg. The arrowheads indicate the glomerulus, while stars highlight the S1-S2 segments of the proximal convoluted tubules (panel A).

Urinary albumin-to-creatinine ratio (ACR) measured in mice exposed to control or HFHS diet in the absence or presence of empagliflozin treatment (1-3-10 mg/kg). Values are means ± SEM for n = 10 randomly selected animals per group. **$p<0.01$ *vs* C; ##$p<0.05$; ###$p<0.001$ *vs* HFHS (panel B).

Figure 4 Effect of empagliflozin on diet-induced NLRP-3 inflammasome in the kidney.

JPET Fast Forward. Published on July 20, 2016 as DOI: 10.1124/jpet.116.235069
This article has not been copyedited and formatted. The final version may differ from this version.

Expression of NLRP-3 (panel A), procaspase-1 and activated caspase-1 (panel B) in the kidney of control and HFHS animals untreated or treated with empagliflozin 1-3-10 mg/kg were evaluated by immunoblotting. Each immunoblot is from a single experiment and is representative of 6-9 randomly selected animals per group. Densitometric analysis of the bands is expressed as relative optical density (O.D.), corrected for the corresponding b-actin contents, and normalized using the related control band. Values are means ± SEM *p<0.05, **p<0.01 and ***p<0.001 vs C; #p<0.05 vs HFHS. Statistical analysis was performed with Kruskal-Wallis test with Dunnes post-hoc test. IL-1β levels were evaluated by ELISA in kidney homogenates of 15 randomly selected animals per group. Values are means ± SEM **p<0.01 vs C; #p<0.05 vs HFHS (panel C).

Figure 5 Effects of empagliflozin treatment on diet-induced liver damage.

Representative pictures (×200 magnification) of hematoxylin-eosin stained on liver sections from control and HFHS animals untreated or treated with empagliflozin 10 mg/kg. The arrowheads underline the portal space; the Acinar Zone 1, where periportal hepatocytes are present, has been indicated (panel A).

Triglycerides (TGs) content in mouse liver. Data are means ± SEM for n = 10 randomly selected animals per group. Statistical analysis was performed with Kruskal-Wallis test with Dunnes post-hoc test. **p<0.01 and ***p<0.001 *vs* C; #p<0.05 *vs* HFHS (panel B).

Figure 6 Effect of empagliflozin on diet-induced NLRP-3 inflammasome in the liver.

Expression of NLRP-3 (panel A), procaspase-1 and activated caspase-1 (panel B) in the liver in control and HFHS animals untreated or treated with empagliflozin 1-3-10 mg/kg were evaluated by immunoblotting. Each immunoblot is from a single experiment and is representative of n = 6-9 animals per experimental group. Densitometric analysis of the bands is expressed as relative optical density (O.D.), corrected for the corresponding β-actin contents, and normalized using the related control band. Values are means ± SEM *p<0.05

and **p<0.01 *vs* C; #p<0.05 *vs* HFHS. Statistical analysis was performed with Kruskal-Wallis test with Dunnes post-hoc test. IL-1β levels were evaluated by ELISA in liver homogenates for n = 15 randomly selected animals per group. Values are means ± SEM. **p<0.01 *vs* C; #p<0.05 vs HFHS (panel B).

Figure 7 Effects of empagliflozin treatment on diet-induced cardiac fat accumulation and NLRP-3 inflammation.

Representative photomicrographs (×40 magnification) of Oil Red O staining of cardiac apex sections from control and HFHS animals untreated or treated with empagliflozin 10 mg/kg (panel A). Triglycerides (TGs) content in mouse cardiac apex (panel B). IL-1β levels in left ventricle from control and HFHS animals untreated or treated with empagliflozin 1-3-10 mg/kg were measured by ELISA (panel C). Data are means ± SEM for n = 8 randomly selected animals per group. For TGs, statistical analysis was performed with Kruskal-Wallis test with Dunnes post-hoc test.

JPET Fast Forward. Published on July 20, 2016 as DOI: 10.1124/jpet.116.235069
This article has not been copyedited and formatted. The final version may differ from this version.

Tables

Table 1. Effect of diet manipulation and empagliflozin treatment

PARAMETER	CONTROL	CONTROL +E10	HFHS	HFHS +E1	HFHS +E3	HFHS +E10
Caloric intake (KJ/die/mouse)[a]	37.16±1.85	41.68±3.51	47.78±7.86***	49.01±5.48***	50.1±6.12***	48.15±6.71***
Energy efficiency (g/MJ)[a]	1.49±0.26	1.04±0.40	2.23±0.68**	1.83±0.64	1.85±0.99	1.05±0.57###
Anatomical						
Weight gain (g)[a]	3.1 ±0.55	2.42±0.93	5.98±1.81***	5.04±1.75**	5.18±2.77**	2.83±1.54###
Liver weight (g)	0.87±0.09	0.85±0.07	1.04±0.16***	1.05±0.14***	1.06±0.13***	0.98±0.08
Kidney weight (g)	0.26±0.02	0.26±0.02	0.30±0.03***	0.32±0.03***	0.32±0.03***	0.32±0.04***
Heart weight (g)	0.11±0.01	0.11±0.01	0.12±0.02	0.13±0.02	0.12±0.02	0.12±0.02
Epididymal fat weight (g)	0.43±0.11	0.36±0.09	1.72±0.53***	1.55±0.57***	1.63±0.75***	1.31±0.36***#
Plasmatic						
Fasting glucose (mg/dl)	113.30±11.79	99.38±24.04	171.3±21.40***	148.6±39.27**#	136.07±25.2###	128.93±21.93###
Insulin (pg/ml)	271.5±105.3	230.2±77.1	481.6±131.9***	356.9± 96.7	422.5 ±130.8*	417.3±100.2*
Homa-IR	1.65±1.03	1.27±0.44	5.04±1.45***	2.47±1.09###	3.19± 0.74#	2.85±0.45###
Total chol (mg/dl)	102.32±24.31	109.73±5.34	138.86±10.89*	126.51±31.51	117.82±18.60	120.91±17.54
LDL chol (mg/dl)	40.67±2.84	42.18±3.84	65.23±5.80*	54.87±20.64	50.19±13.31	52.27± 12.27
HDL chol (mg/dl)	43.68±4.13	48.30±4.28	53.26±6.27	50.18±8.20	49.64±2.42	48.55±11.94
Triglycerides (mg/dl)	86.2±18.3	83.3±9.5	108.5±14.6	103.1±8.2	91.1±30.2	95.4±11.3

*[a] average from 8 to 16 week; *p <0.05; **p <0.01; ***p<0.001 vs CONTROL; #p <0.05; ###p<0.001 vs HFHS*

Figure 1

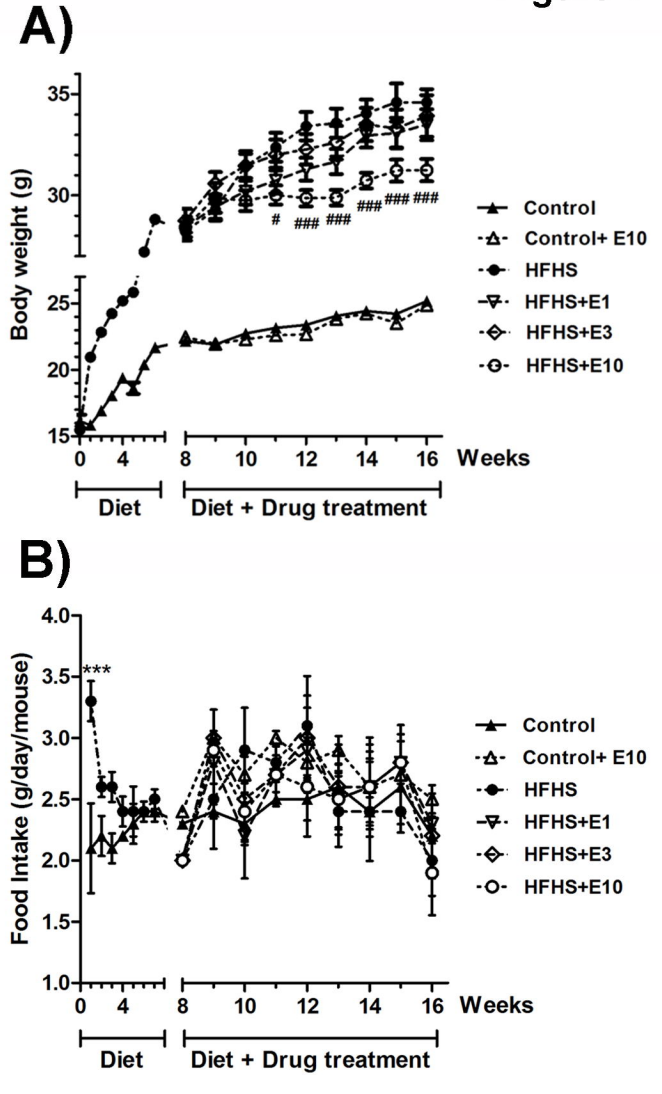
A)
Body weight (g)
35
30
25
20
15
0
4
8
10
12
14
16
Weeks
Diet
Diet + Drug treatment
#
###
###
###
###
###
Control
Control+ E10
HFHS
HFHS+E1
HFHS+E3
HFHS+E10
B)
Food Intake (g/day/mouse)
4.0
3.5
3.0
2.5
2.0
1.5
1.0
***
0
4
8
10
12
14
16
Weeks
Diet
Diet + Drug treatment
Control
Control+ E10
HFHS
HFHS+E1
HFHS+E3
HFHS+E10

Figure 2

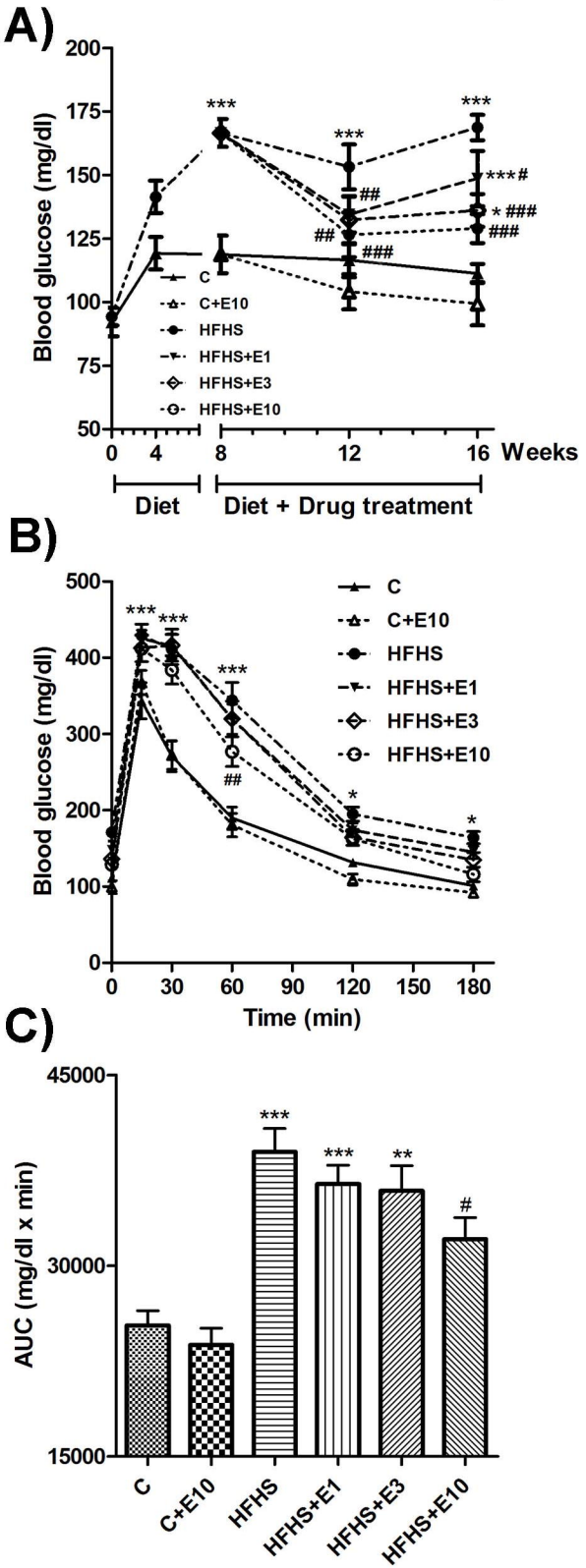
A)
Blood glucose (mg/dl)
200
175
150
125
100
75
50
0
4
8
12
16
Weeks
C
C+E10
HFHS
HFHS+E1
HFHS+E3
HFHS+E10
Diet
Diet + Drug treatment
B)
Blood glucose (mg/dl)
500
400
300
200
100
0
0
30
60
90
120
150
180
Time (min)
C)
AUC (mg/dl x min)
45000
30000
15000
C
C+E10
HFHS
HFHS+E1
HFHS+E3
HFHS+E10

Figure 3

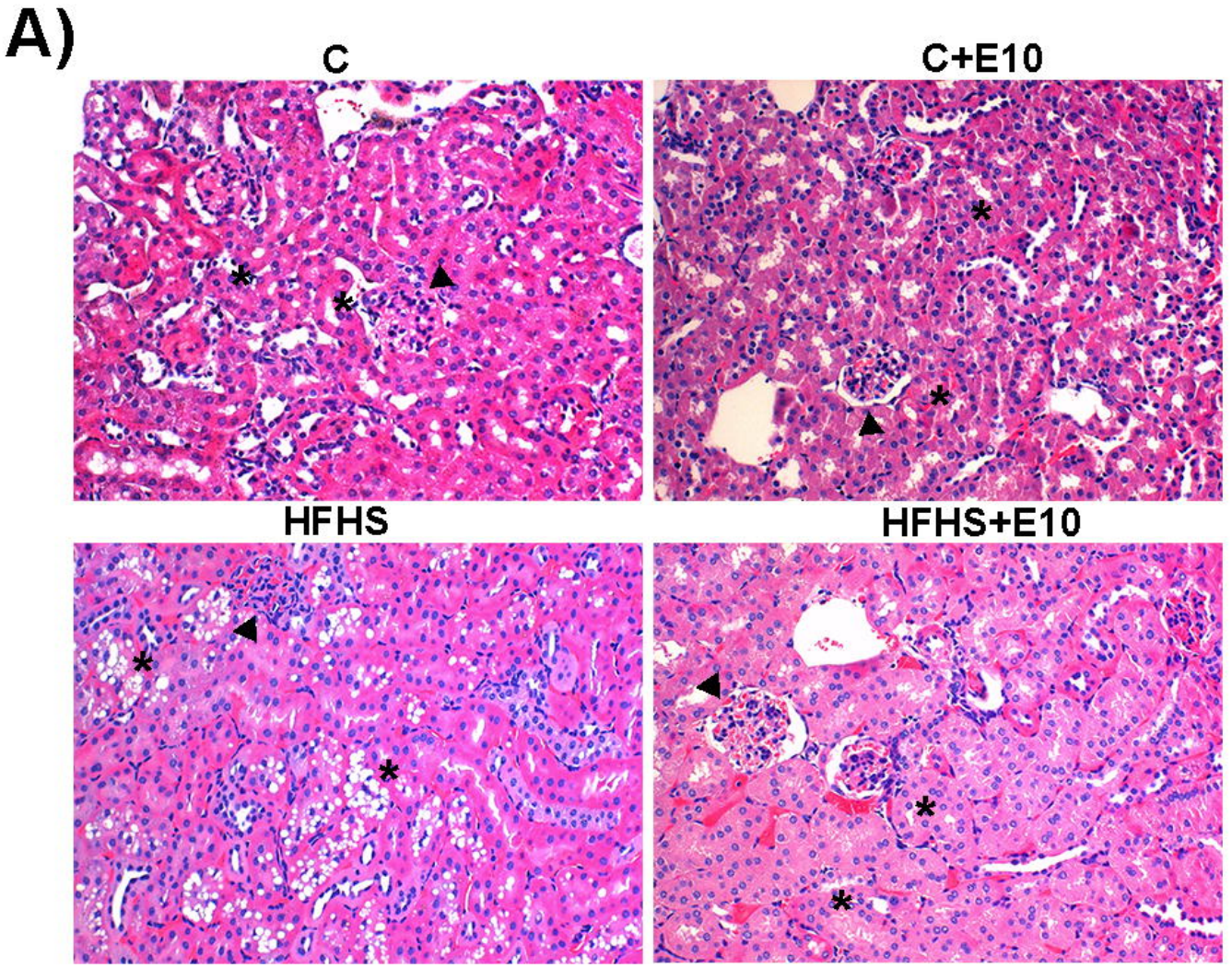
A)
C
C+E10
HFHS
HFHS+E10

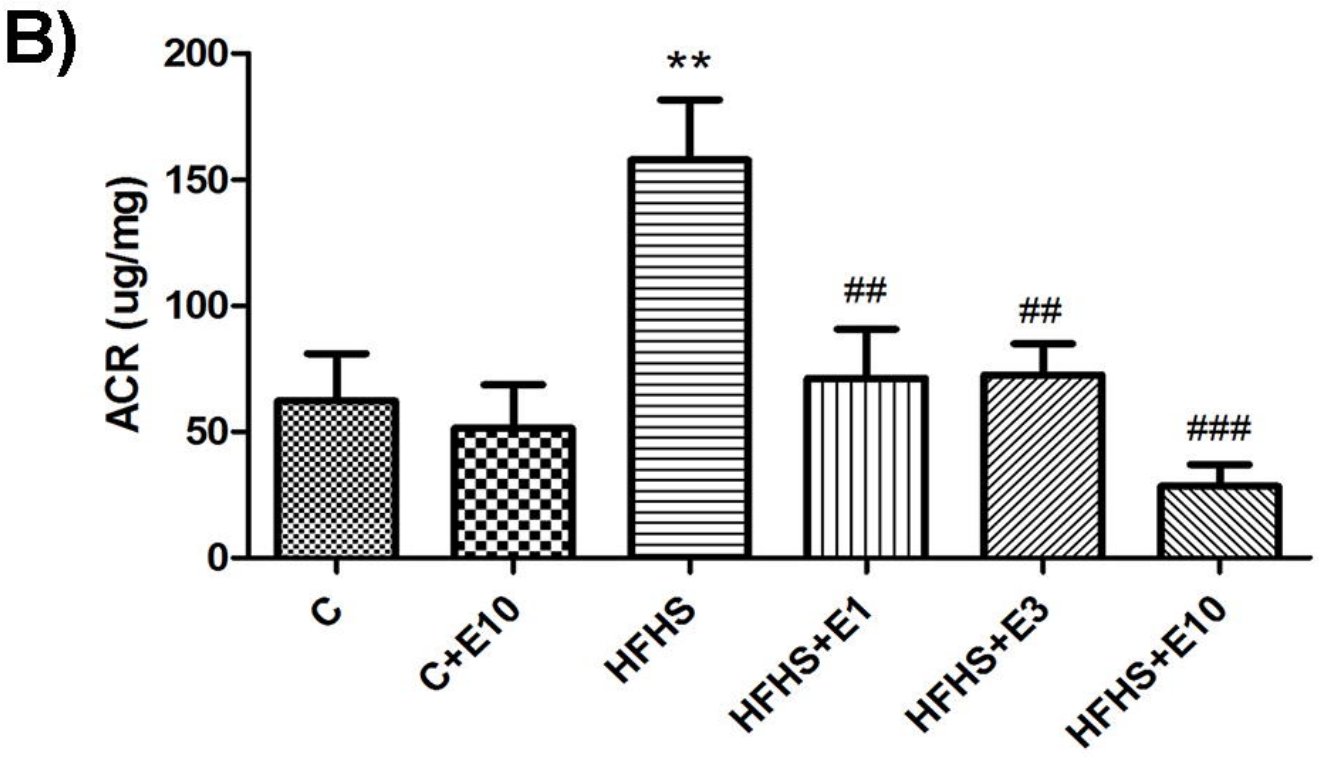
B)
ACR (ug/mg)
200
150
100
50
0
**
##
##
###
C
C+E10
HFHS
HFHS+E1
HFHS+E3
HFHS+E10

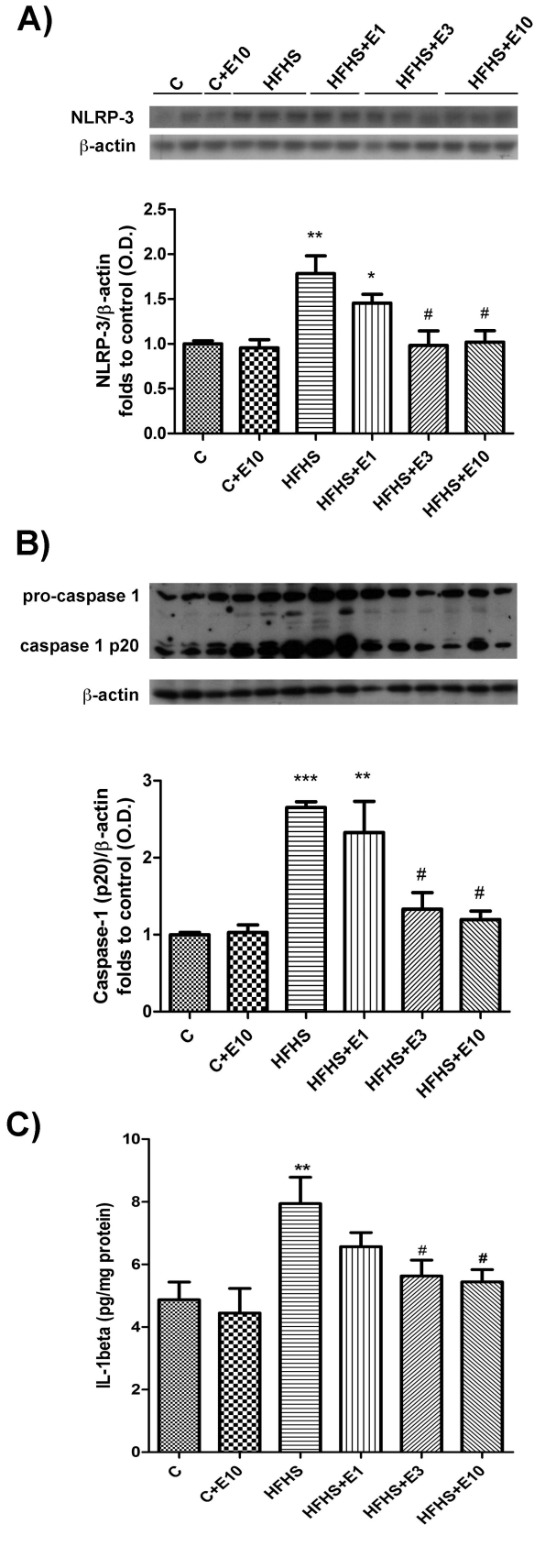
A)
C
C+E10
HFHS
HFHS+E1
HFHS+E3
HFHS+E10
NLRP-3
β-actin
NLRP-3/β-actin folds to control (O.D.)
2.5
2.0
1.5
1.0
0.5
0.0
**
*
#
#
C
C+E10
HFHS
HFHS+E1
HFHS+E3
HFHS+E10
B)
pro-caspase 1
caspase 1 p20
β-actin
Caspase-1 (p20)/β-actin folds to control (O.D.)
3
2
1
0
***
**
#
#
C
C+E10
HFHS
HFHS+E1
HFHS+E3
HFHS+E10
C)
IL-1beta (pg/mg protein)
10
8
6
4
2
0
**
#
#
C
C+E10
HFHS
HFHS+E1
HFHS+E3
HFHS+E10

Figure 5

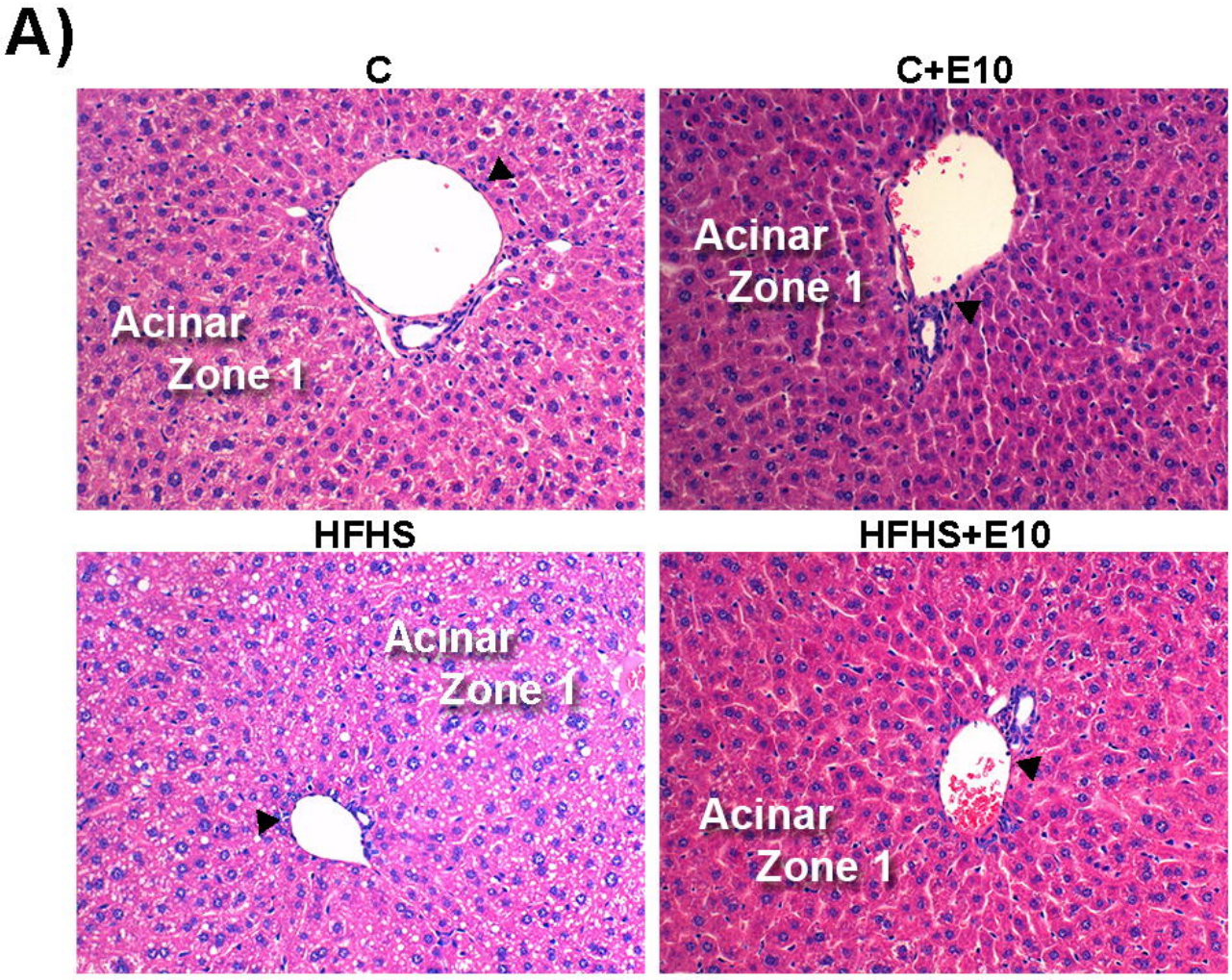
A)
C
C+E10
HFHS
HFHS+E10
Acinar Zone 1
Acinar Zone 1
Acinar Zone 1
Acinar Zone 1

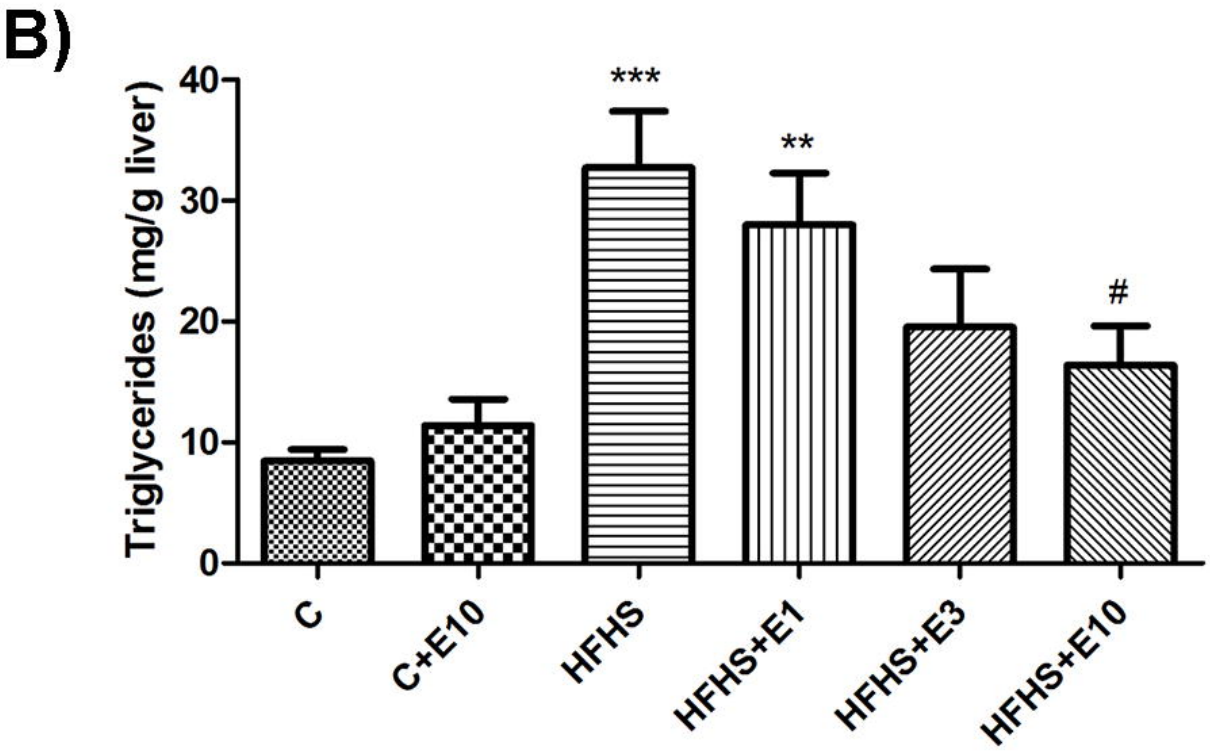
B)
Triglycerides (mg/g liver)
40
30
20
10
0
***
**
#
C
C+E10
HFHS
HFHS+E1
HFHS+E3
HFHS+E10

A)

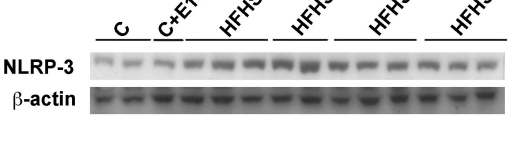
C
C+E10
HFHS
HFHS+E1
HFHS+E3
HFHS+E10
NLRP-3
β-actin

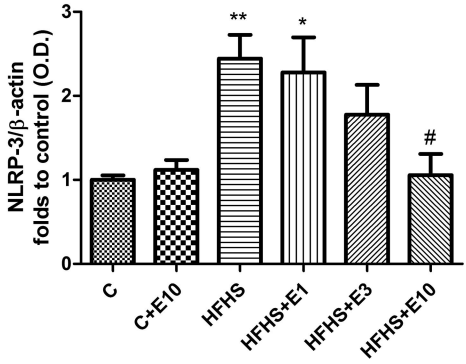
NLRP-3/β-actin folds to control (O.D.)
3
2
1
0
**
*
#
C
C+E10
HFHS
HFHS+E1
HFHS+E3
HFHS+E10

B)

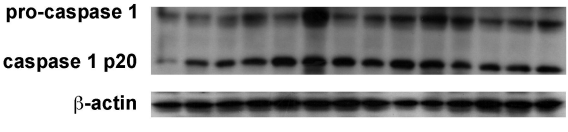
pro-caspase 1
caspase 1 p20
β-actin

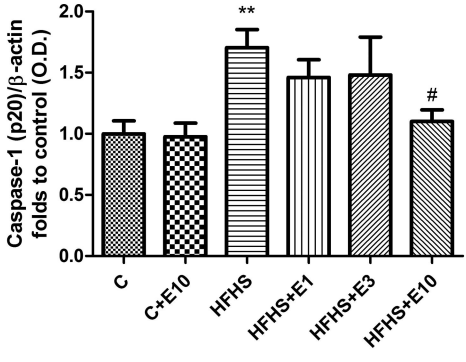
Caspase-1 (p20)/β-actin folds to control (O.D.)
2.0
1.5
1.0
0.5
0.0
**
#
C
C+E10
HFHS
HFHS+E1
HFHS+E3
HFHS+E10

C)

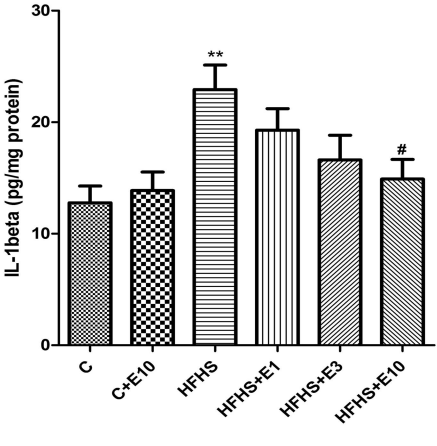
IL-1beta (pg/mg protein)
30
20
10
0
**
#
C
C+E10
HFHS
HFHS+E1
HFHS+E3
HFHS+E10

A)

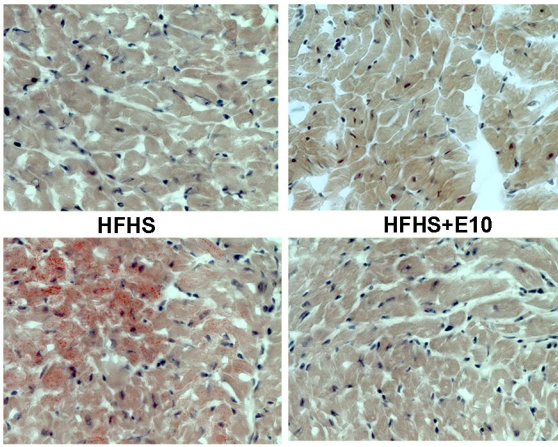
C
C+E10
HFHS
HFHS+E10

B)

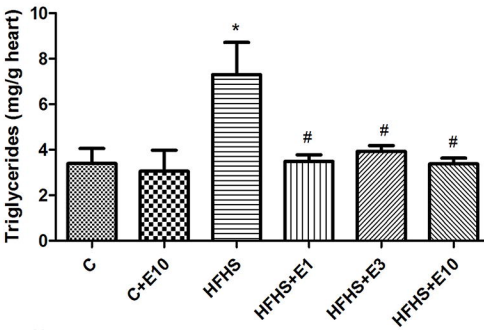
Triglycerides (mg/g heart)
0
2
4
6
8
10
*
#
#
#
C
C+E10
HFHS
HFHS+E1
HFHS+E3
HFHS+E10

C)

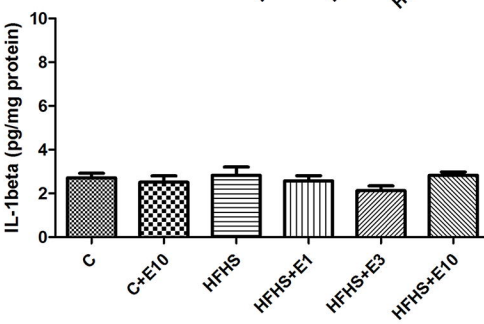
IL-1beta (pg/mg protein)
0
2
4
6
8
10
C
C+E10
HFHS
HFHS+E1
HFHS+E3
HFHS+E10